Materials Science-Poland, Vol. 25, No. 1, 2007

Fabrication of Al–4.5% Cu alloy with fly ash metal matrix composites and its characterization

K.V. MAHENDRA[1*], K. RADHAKRISHNA[2]

[1]Department of Mechanical Engineering, New Horizon College of Engineering, Outer Ring Rd., Panathur Post Bangalore-560087, Karnataka State, India

[2]Mechanical Department BMS College of Engineering, Bangalore-560019, India

Metal matrix composites (MMCs) are engineered materials, formed by the combination of two or more dissimilar materials (at least one of which is a metal) to obtain enhanced properties. In the present investigation, an Al–4.5% Cu alloy was used as the matrix and fly ash as the filler material. The composite was produced using conventional foundry techniques. The fly ash was added in 5%, 10%, and 15 wt. % to the molten metal. The composite was tested for fluidity, hardness, density, mechanical properties, impact strength, dry sliding wear, slurry erosive wear, and corrosion. Microstructure examination was done using a scanning electron microscope to obtain the distribution of fly ash in the aluminium matrix. The results show an increase in hardness, tensile strength, compression strength, and impact strength with increasing the fly ash content. The density decreases with increasing fly ash content. Resistance to dry wear and slurry erosive wear increases with increasing fly ash content. Corrosion increases with increasing fly ash content.

Key words: *wear; metal matrix composite; fly ash; corrosion; aluminium alloy*

1. Introduction

Traditional materials do not always provide the necessary properties under all service conditions. Metal matrix composites (MMCs) are advanced materials resulting from a combination of two or more materials (one of which is a metal and the other a non-metal) in which tailored properties are realized. They have received considerable attention in recent years due to their high strength, stiffness, and low density. Data related to mechanical properties, wear, microstructure, etc., have been cited in the literature. It has been reported that particle size and wear parameters (sliding speed, material property, normal load) influence the wear of the material [1–3]. A variety of particles such as mica, Al_2O_3, graphite, and SiC have been used as reinforcement materials with aluminium alloys [4–8] as the matrices. It appears that stir

*Corresponding author, e-mail: mahendrakv@rediffmail.com

casting is one of the methods for producing composites. The use of fly ash as a reinforcement material [9] results in improvement of mechanical properties of the composite. An extensive review on dry sliding wear characteristics of composites based on aluminium alloy was undertaken by Sannino et al. [10] and of their abrasive wear behaviour by Deuis [11]. Fly ash was separated into cenosphere and precipitator fly ash. The use of precipitator fly ash in aluminium decreases the density of composites and increases their wear resistance [12]. In slurry erosive wear, the effect of the impingement angle and velocity on the erosion rate depends on particle size and amount of particulates. It has been reported that the erosion rate increases with increasing particle size up to a point, beyond which it is not significantly affected by the size. It was reported that corrosion increases with increasing particulates in composites [13]. Bienias et al. [14] reported the pitting corrosion behaviour and corrosion kinetics of Al alloy with precipitator fly ash (9 vol %, 75–100 μm) composites. It was found that fly ash particles lead to an enhanced pitting corrosion of the composite in comparison to unreinforced matrix.

In the present investigation, Al–4.5% Cu alloy with fly ash (as received from a thermal power plant) as particulates were successfully fabricated using the stir casting method. Fluidity, mechanical properties, dry sliding wear, slurry erosive wear, and the corrosion behaviour of the MMCs were investigated.

2. Experimental

Aluminium with 4.5% Cu was selected as the matrix material. The chemical composition, analysed by a Bairdas DV-6S optical emission spectrometer, is given in Table 1. Fly ash was used as the reinforcement and its composition is given in Table 2. The average particle size was found to be 10 μm. The density of fly ash was found to be 2.09 g/cm^3. Fig. 1 shows SEM micrographs of fly ash particulates.

Table 1. Chemical composition of Al–4.5% Cu alloy

Cu	Mg	Si	Fe	Mn	Ni	Pb	Sn	Ti	Zn	Al
4.52	0.066	0.538	0.663	0.131	0.075	0.029	0.021	0.013	0.118	balance

Table 2. Chemical composition of fly ash in weight percentages

Al_2O_3	SiO_2	Fe_2O_3	TiO_2	Loss on ignition
30.40	58.41	8.44	2.75	1.43

The synthesis of the composite was carried out by stir casting. The ingots of Al–4.5% Cu alloy were taken in a graphite crucible and melted in an electric furnace. The temperature was slowly raised to 850 °C. The melt was degassed at 800 °C using a solid dry hexachloroethane (C_2Cl_6, 0.5 wt. %) degasser. The molten metal was stirred to create a vortex and the particulates were introduced. The degassed molten metal was placed below the stirrer and stirred at approximately 600 rpm. The preheated fly ash particles were slowly added into the melt. Small pieces of Mg (0.5 wt. %)

were added to the molten metal to ensure good wettability of particles with the molten metal. The percentage of fly ash added was 5, 10, or 15 wt. %. The stirred dispersed molten metal was poured into preheated S.G. iron moulds 25, 50, or 75 in diameter and 200 mm hight, and cooled to room temperature.

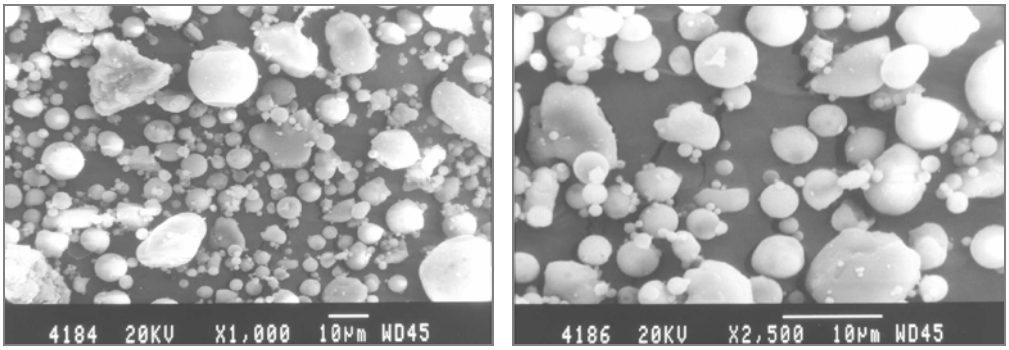

Fig. 1. SEM of fly ash particulates

The flowability characteristic of the molten metal was assessed using two types of fluidity tests, the spiral and strip ones. The total length of the metal flowing inside the mould cavity was taken as a measure of fluidity.

Composites produced were subjected to solutionisation and age hardening (T6). The castings were heated to 525 °C and held for 17 hours, quenched in warm water, then reheated to 175 °C and held for 18 hours. They were sectioned and test samples were prepared for various tests. The densities of the specimens were measured using the Archimedes principle. Their hardness was determined using the Brinnel hardness tester. The load of 500 kg using a 10 mm steel ball indenter was used to measure the hardness. The microstructure of the MMCs was observed under a scanning electron microscope (SEM) at various locations across the specimen to examine the distribution of fly ash in the matrix.

Tensile and compression strengths were determined using a 20 kN computerised UTM with an electronic extensometer as per ASTM E-8 standards. Online plotting of load versus extension was done continuously through a data acquisition system. The impact strength of castings was tested using a standard impact testing machine using Izod and Charpy specimens. The Izod test is carried out by a pendulum-type testing machine, which employs a cantilever test specimen 75 mm long with a 10×10 mm^2 cross section, having a standard 45° notch 2 mm deep. The Charpy test employs a notched specimen $10\times10\times55$ mm^3 in size with a U notch.

Dry sliding wear test. Specimens 5 mm in diameters and 20 mm long were used for the dry sliding wear tests. The tests were carried out using a computerized pin on a disc wear testing machine under ambient temperature conditions on specimens for normal loads of 4.9, 9.8, 14.7, and 19.6 N, and for a constant track velocity of 80 m/sec.A hardened steel disc (60 HRc) was used as the counterface. The wear of the

specimen and friction were measured directly using sensors. The wear tracks on the specimen were observed under a SEM to examine the effect of the percentage of particulate on the wear behaviour of the MMCs.

Slurry erosive wear test. Slurry erosive wear was made using a bolt-shaped specimen7 mm in diameter. A slurry of silica sand and distilled water in the ratio 1:2 with different pH values was used. The bolt specimen was rotated in the slurry at 1170 rpm for 24 hours, then washed, dried, and weighed with a digital balance every 2 hours. The loss of weight was recorded for each time interval. The experiment was repeated for neutral, basic, and acidic conditions of the slurry.

Fog corrosion test. Thin rectangular specimens of 25.4×101.6×6 mm^3 dimensions were exposed to a fog atmosphere of salt solution in a closed chamber. The specimens were prepared with a good surface finish, cleaned and used. The test was carried out as per ASTM B-117 standards. The temperature of the salt bath was maintained at 25 °C and air was bubbled through the bath under the pressure of 0.69 bar. Every 3 hours the specimens were taken out, cleaned, dried, and weighed accurately. The total testing time was 48 hours.

3. Results and discussion

Figure 2 shows the effect of fly ash content on the fluidity of composites. It was observed that with an increasing percentage of fly ash particulates the fluidity length

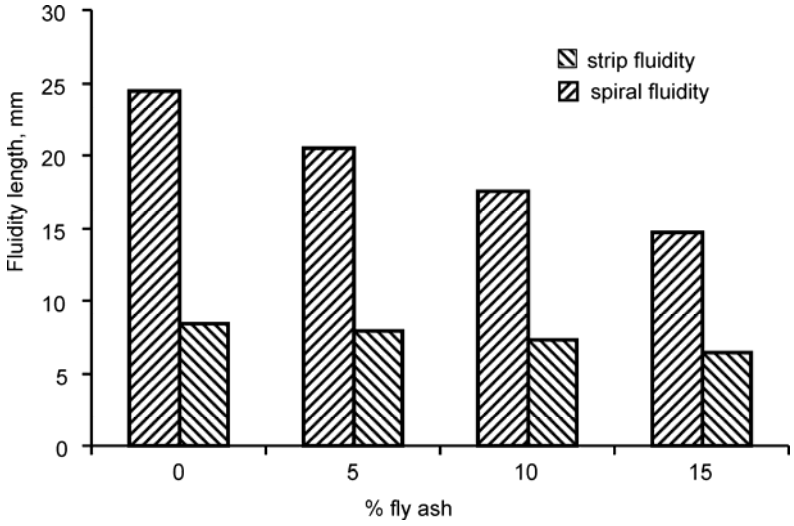

Fig. 2. The effect of fly ash on fluidity of composite

decreases. This may be due to an obstruction to the flow of molten metal by fly ash particulates, in turn due to an increase in the viscosity of the base alloy as a result of

the suspension of fly ash particles. Base metal shows a better fluidity than composites in both strip and spiral fluidity.

The density decreases with an increasing percentage of particulates (Fig. 3). Since the density of fly ash was 2.09 g/cm^3, the overall density of fly ash composite was decreased. The hardness increases with an increasing percentage of particulates. This may be due to the presence of hard fly ash particulates.

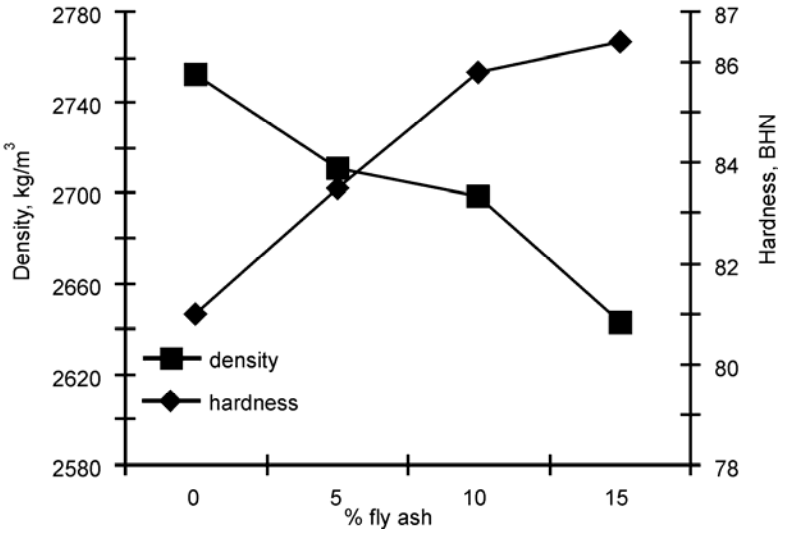

Fig. 3. The density and hardness of composites

The microstructure of MMCs clearly shows a uniform distribution of fly ash in the matrix (Fig. 4), with no void and discontinuities observed. There was good interfacial bonding between the fly ash particles and matrix material. Figure 5 shows a photomicrograph of a single fly ash particle in the matrix, displaying a good bonding.

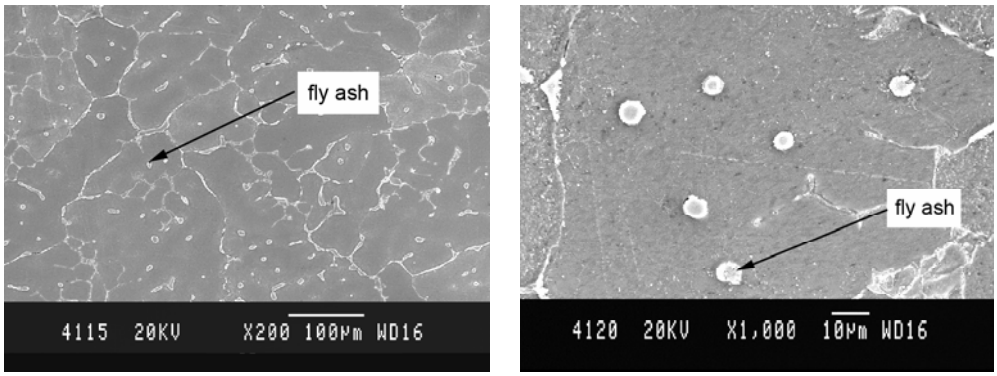

Fig. 4. Photomicrograph of castings 50 mm in diameter with 5% fly ash

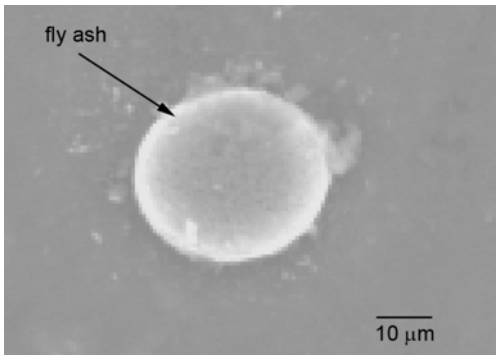

Fig. 5. Enlarged view of a single fly ash particle

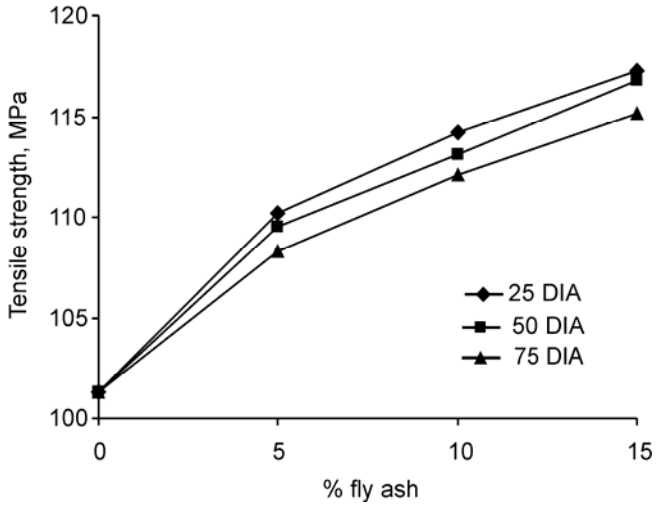

Fig. 6. The tensile strength of composites

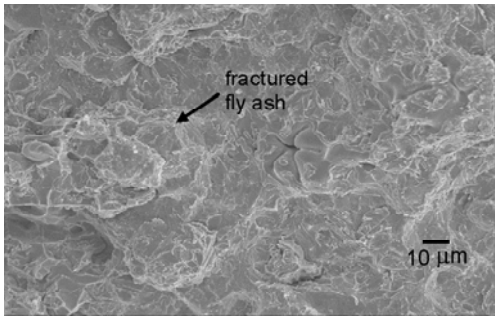

Fig. 7. The tensile fractured surface of the composite

The tensile strength (Fig. 6) increases with an increasing percentage of fly ash particulates. Castings with smaller cross sections exhibit higher tensile strengths than those with larger cross sections. This may be due to a faster heat transfer from the mould, resulting in a finer grain structure of the castings. The fracture of fly ash particulates can be seen in the SEM photomicrograph of 5% fly ash composite (Fig. 7).

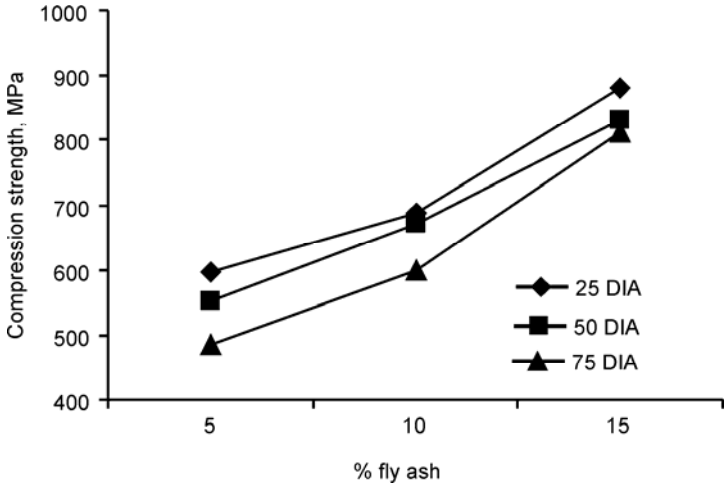

Fig. 8. Compression strengths of composites

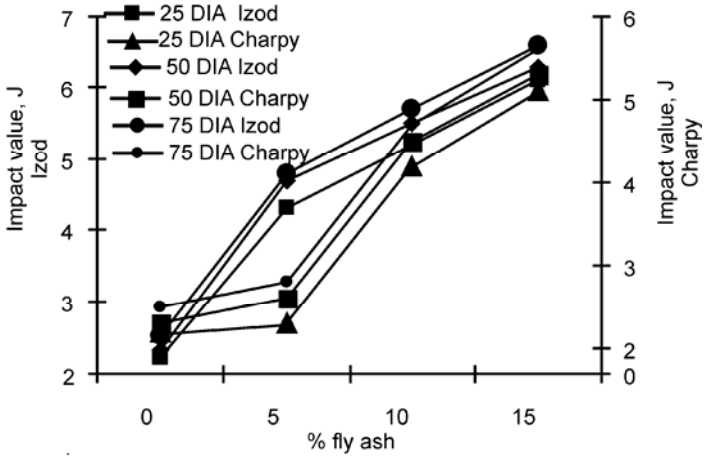

Fig. 9. Izod and Charpy impact strengths of composites

Similarly, compression strength (Fig. 8) increases with increasing percentage of fly ash particulates. This may be due to the hardening of the base alloy by fly ash particulates. The impact strength (Fig. 9) also increases with increasing fly ash content. This may be due to the presence of hard fly ash particulates. The impact strength shows higher values for 10% and 15% fly ash composites than the base alloy.

3.1. Dry sliding wear

Figure 10 shows the results of dry sliding wear behaviour for MMCs with 5, 10, and 15% fly ash content. It was observed that wear decreases with increasing fly ash content. This may be due to the abrasive nature of fly ash. Since the average particle

size of fly ash lies in the range 1–10 μm, the extent of particles pulled out from the surface was smaller. With increasing fly ash content, the amount of particle present strengthens the matrix and hence more wear resistance is observed.

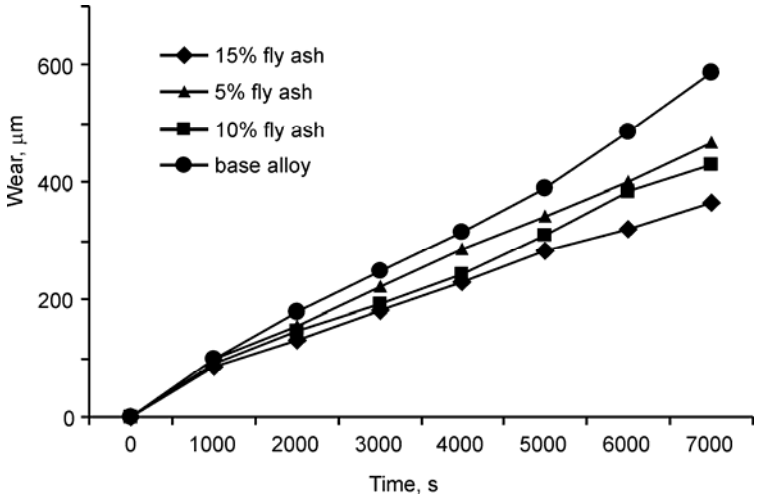

Fig. 10. Wear vs. time at various fly ash percentages at the 4.9 N load of castings 50 mm in diameter.

It was observed that with increasing load wear increases for normal loads of 4.9, 9.8, 14.7, and 19.6 N. Castings with smaller diameters exhibit less wear than castings with the larger ones. It was also observed that with increasing fly ash content there was a decrease in frictional force and the coefficient of friction (Tables 3, 4).

Table 3. Average values of frictional force N for fly ash composites with the addition of particulates, after 120 minutes

Load, N	Fly ash content, %			
	0	5	10	15
4.9	1.8	0.22	0.18	0.11
9.8	3.2	1.9	1.4	1.1
14.7	5.6	4.8	4.1	3.2
19.6	5.9	5.8	5.1	4.6

Table 4. Average values of the coefficient of friction μ for fly ash composites with addition of particulates after, 120 minutes

Load, N	Fly ash content, %			
	0	5	10	15
4.9	0.32	0.28	0.25	0.22
9.8	0.31	0.27	0.23	0.21
14.7	0.3	0.22	0.18	0.16
19.6	0.28	0.12	0.11	0.10

Figure 11 shows the worn surface of 5% fly ash composite (25 mm in diameter) under the normal load of 4.9 N. It can be seen that the ploughing and scoring along the sliding direction is enhanced. When compared to the base alloy, the wear scars are smaller due to the presence of fly ash particulates. This shows that the presence of fly ash in the matrix offers a resistance to wear. The fractured fly ash particles are seen in the SEM photomicrographs.

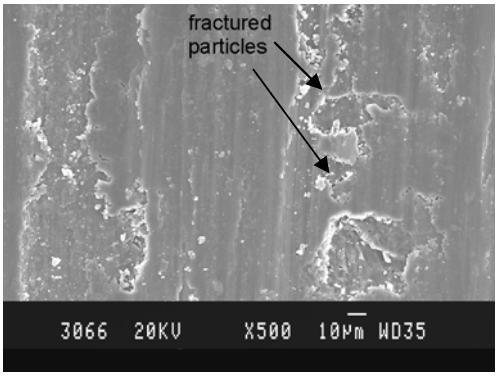

Fig. 11. A worn-out surface of 5% fly ash composite at 4.9 N (25 mm in diameter)

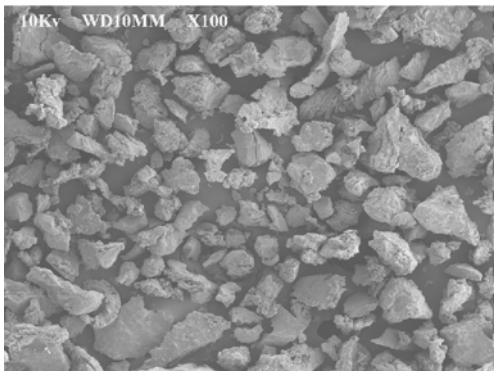

Fig. 12. The wear debris of a composite

The worn debris particles are likely to act as third body abrasive particles. The fly ash particles trapped between the specimen and counterface cause microploughing on the contact surface of the composite. The continuous longitudinal lines parallel to the sliding direction on the worn surfaces of the composites probably result from the ploughing action of the fly ash particles. At higher loads, composites show delamination, due to which the material loss in the form of plate-like debris takes place. The additional abrasive wear (microploughing) component of the sliding wear caused by fly ash particles may be the reason for the marginal decrease in wear rate of 15% fly ash reinforced composites compared to composites reinforced with 10% and 5% fly ash. Figure 12 shows the wear debris of MMCs. The volume of wear debris increases with increasing normal load, resulting in greater wear loss.

3.2. Slurry erosive wear

Figure 13 shows the time dependence of weight loss for erosive wear in an acidic medium. It was observed that with an increasing percentage of fly ash particulates the slurry erosive wear decreases. Erosive wear in the case of a basic medium is larger than in an acidic one. The erosion of MMCs takes place by the impact of abrasives present in the slurry. Initially, the corrosion of the matrix takes place by the oxidation reaction when Al^{3+} ions are released from the matrix to the slurry. Due to this, more

surface area is exposed to the slurry and causes further removal of the matrix and hence a higher loss of weight in the initial stage. Further in time, the slurry adjacent to the specimen surface becomes saturated with Al^{3+}, resulting in a reduction of the pH of the slurry. As a result, the dissolution rate of Al^{3+} in the slurry is reduced and the excess of Al^{+3} ions are deposited over the specimen surface, reacting with OH^- ions to form $Al(OH)_3$. This passive layer slows the rate of weight loss. SEM photomicrographs of slurry abrasive wear specimens show pitting in few places (Fig. 14).

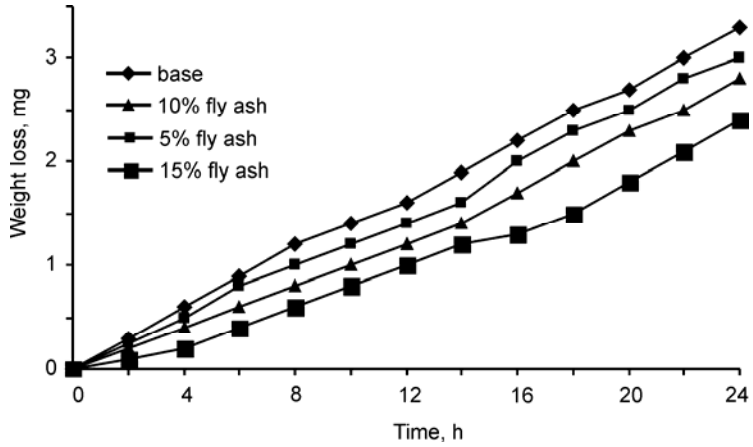

Fig. 13. Slurry erosive wear – acidic medium
(castings 50 mm in diameter)

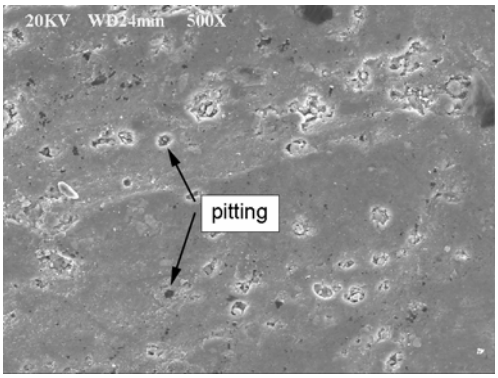

Fig. 14. SEM of the worn surface
of a composite under acidic conditions

3.3. Fog corrosion

Figure 15 shows weight loss versus time for fly ash composites tested at various temperatures for castings 50 mm in diameter. The temperature has an effect on the corrosion. It was observed that with increasing temperature corrosion increases, and the base alloy shows less corrosion than the composites in all the cases. It was also observed that corrosion increases with an increasing percentage of fly ash particu-

lates. The formation of an aluminium oxide layer is visible within 20 hours of commencing the test. Pits were formed in the specimens due to corrosion.

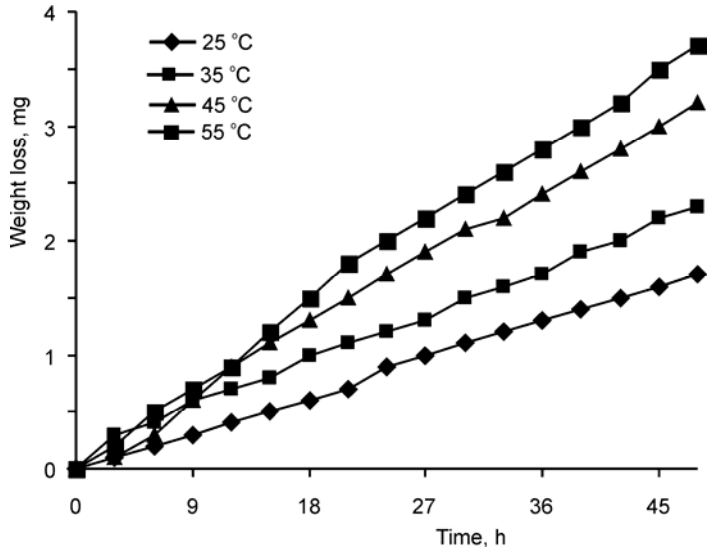

Fig. 15. Weight loss versus time at various temperatures of castings 50 mm in diameter (10% fly ash)

As is evident from the SEM photographs (Fig. 16), there was a build-up of corroded particle debris in the pits. The interfaces between reinforcement and matrix material, where the matrix surface is broken, will act as pit initiators. Since pits initiate at flaws and interfaces between matrix aluminium and reinforced particles are flaws, the metal is pitted by aerated sodium chloride solution.

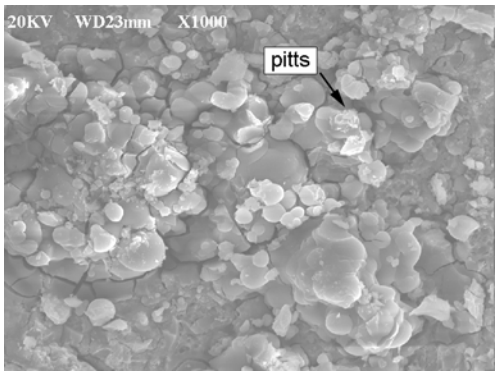

Fig. 16. SEM photomicrograph of a corroded surface (5% fly ash)

The rapid dissolution of aluminium occurs within pits, while oxygen reduction takes place on adjacent surfaces. The rapid dissolution of aluminium within pits tends to produce an excess of positive charge in these areas, resulting in the migration of

chloride ions to maintain electroneutrality. Thus, there will be high concentrations of hydrogen ions in pits as a result of hydrolysis, and this process accelerates with time.

4. Conclusions

MMCs containing up to 15% fly ash particles were easily fabricated. A uniform distribution of fly ash was observed in the matrix. The fluidity and density of the composites decreases, whereas the hardness increases with an increasing percentage of the fly ash particulates. The tensile strength, compression strength, and impact strength increase with an increasing percentage of fly ash particulates. The dry sliding wear resistance increases with an increasing percentage of fly ash. In the slurry erosive wear test, the resistance to wear increases with increasing fly ash content. The wear is enhanced in the case of basic media compared to acidic and neutral media. Corrosion increases with an increasing percentage of fly ash content. The MMC produced can be used for bearing applications, because of its good wear resistance.

References

[1] EYRE T.S., Tribol. Int., (1976), 203.
[2] BHANSALI K.J., MEHRABIAN R., J. Metals, 34 (1982), 30.
[3] HOSKING F.M., PORTILLO F.F., WUNDERLIN R., MEHRABIAN R., J. Mater. Sci., (1982), 477.
[4] DEONATH S.K., BHAT R.T., ROHATGI P.K., J. Mater. Sci., (1980), 1241.
[5] MAJUMDAR B.C., YEGNESHWARAN A.H., ROHATGI P.K., Mater. Sci. Eng., 68 (1984), 885.
[6] POZA P., LLORCA J., Mater. Sci. Eng., A206 (1996), 183.
[7] PRADER P., DEGISCHER H.P., Mater. Sci. Technol., 16(2000), 893.
[8] IAN J.H., Metal Powder Rep., 10(1990), 689.
[9] ROHATGI P.K., GUO R.Q, J. Metall. Mater. Trans. B, 298 (1998), 519.
[10] SANNINO A.P., RACK H.J, Wear, 216 (1995), 1.
[11] DEUIS R.L., SUBRAMANIAN C., YELLUP J.M., Wear, 201 (1996), 132.
[12] GUO R.Q., ROHATGI P.K., Metal. Mater. Trans. B, 29B (1998), 519.
[13] HIHARA L.H., LATANISION R.M, Int. Mater. Rev., 39 (1994), 245.
[14] BIENIAS J., WALCZAK M., SUROWSKA B., SOBCZAK J., J. Optoelectronics Adv. Mater., 5, (2003), 55.

Received 21 July 2005
Revised 22 May 2006